Macromolecules
ARTICLE

Macromolecules **2010**, *43*, 2219–2227 **2219**
DOI: 10.1021/ma902802s

Role of Bimolecular Homolytic Substitution (S_H2) Reactions in Free Radical Photopolymerization Under Air

Mohamad El-Roz, Mohamad-Ali Tehfe, Jacques Lalevée,* Bernadette Graff, Xavier Allonas, and Jean Pierre Fouassier

Department of Photochemistry, CNRS, University of Haute Alsace, Ecole Nationale Supérieure de Chimie de Mulhouse, 3 rue Alfred Werner, 68093 Mulhouse Cedex, France

Received December 19, 2009; Revised Manuscript Received January 22, 2010

ABSTRACT: A set of multivalent atom-containing amines (e.g., tetrakis(dimethylamido)silane, tetrakis-(dimethylamido)tin(IV), tetrakis(diethylamido)titanium(IV), tetrakis(dimethylamido)zirconium(IV), and 1,3,5-triaza-7-phosphaadamantane) are proposed as new coinitiators in Type II photoinitiating systems (based, for example, on benzophenone) and additives for Type I photoinitiators (such as phenyl bis(2,4,6-trimethylbenzoyl)phosphine oxide and 2-hydroxy-2-methyl-1-phenyl-1-propanone) for free radical photopolymerization under air. The polymerization rates (Rp's) were determined under experimental conditions where a strong detrimental oxygen effect is expected, that is, both under low light intensity and in thin low viscosity monomer samples. The remarkable performance achieved under air (up to a 100- and a 5-fold increase in Rp and final conversion (%), respectively) lies on the presence of a bimolecular homolytic substitution (S_H2) reaction that allows us to convert peroxyls into new initiating radicals efficiently. The mechanisms are investigated by laser flash photolysis (LFP) and electron spin resonance (ESR) experiments.

Introduction

In the last decades, free radical photopolymerization (FRP) reactions have attracted special attention because of their applications and inherent advantages over other polymerization processes.[1−5] Nevertheless, FRP is known to be highly affected by oxygen, which deactivates the photoinitiator (PI) excited states and reacts with the initiating as well as the growing polymer radicals to form peroxyls.[6−11] These latter radicals are stable and do not readily reinitiate the polymerization process. Several ways have been introduced to overcome the effect of the oxygen inhibition, for example, use of high-intensity irradiation sources, use of inert environment, and elimination of oxygen prior to polymerization.[6−8,12] The addition of thiols and amines has been also proposed to decrease the detrimental oxygen effect.[5,6,13−15] Oxygen inhibition usually results in the formation of an unpolymerized layer at the top surface of the sample where the diffusion of oxygen from the surrounding environment is faster than its consumption during the polymerization process.

Recently, we have proposed silanes as highly efficient coinitiators (coI) structures for FRP.[10] Their enhanced efficiency under air was mainly ascribed to the presence of hydrogen abstraction reactions that convert inefficient peroxyls into reactive new silyl radicals (Scheme 1). Reaction 1 in Scheme 1 (by changing H-SiR′R″R‴ for an amine) was also postulated many years ago to account for the effect of amines toward oxygen in FRP,[6,13] but the kinetics of this process, as recently investigated,[10] really seems not to be so favorable.

The aim of the present article is to introduce a new concept for the improvement of FRP under air. This is achieved through the use of a bimolecular homolytic substitution reaction (S_H2). The S_H2 reactions that are well-known in radical chemistry[16] correspond to the addition of a radical ($R_1^•$) to a compound (A-R_2) leading to the formation of a new $R_2^•$ radical (Scheme 2). S_H2's

Scheme 1. Silane Additive Effect

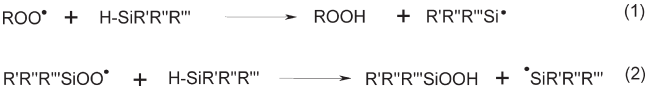

Scheme 2. Mechanism for the S_H2 Reaction

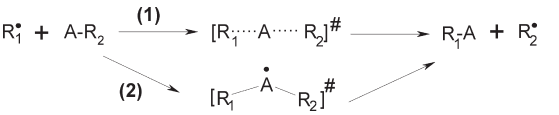

are encountered as elementary steps in many chemical reactions involving various types of radicals ($R_1^•$), mainly *t*-BuO•, $Me_2N^•$, and Me•.[16] They generally require a compound (A-R_2) containing a multivalent saturated atom (A), for example. Si, Sn, S, Se, Te, Mg, Hg, B, P, Zr, and Ti. Depending on the stability of the transition state (TS) that reflects the nature of the multivalent atoms, S_H2 can proceed[16] via either a concerted TS mechanism (direct S_H2) or a radical intermediate TS mechanism (stepwise S_H2).

To the best of our knowledge, the S_H2 potential has not been mentioned before in FRP. The basic idea consists here in applying the S_H2 reaction to convert a peroxyl ($R_1^•$ standing for a peroxyl in Scheme 2) into a new initiating radical ($R_2^•$). As a consequence, this S_H2 process should be useful to overcome the oxygen inhibition. Examples of S_H2's based on ROO• are rather scarce in the literature because of the high stability of these radicals.[16] Moreover, A-R_2 in Scheme 2 should be a carefully selected compound because the S_H2 reaction must be thermodynamically favorable. In our previous studies,[10] silanes were not involved in such a process because the hydrogen abstraction (Scheme 1) was easier and ruled out the competition with another reaction such as S_H2. The direct addition of peroxyls through the S_H2 process

*Corresponding author. E-mail: j.lalevee@uha.fr.

Published on Web 02/09/2010

Scheme 3. Investigated Compounds

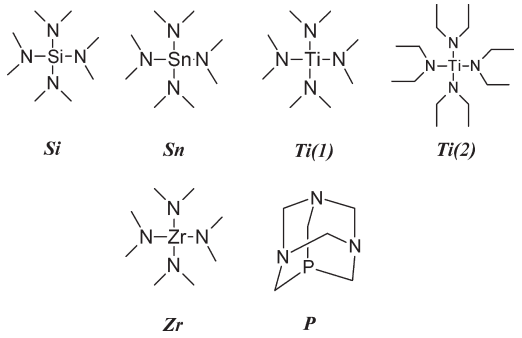

to particular Si, Ti, Zr, and P multivalent atom-containing systems was already documented.[16]

In this work, new coinitiators based on a multivalent-atom-containing structure (MACS) such as various metal(IV) amines are proposed (Scheme 3). In MACS, the amine function is decisive for an efficient generation of initiating radicals through a hydrogen abstraction process when incorporated in a Type II photoinitiating system (PI/MACS), whereas the metal center is highly attractive for the S_H2 reaction in MACS containing both Type I and Type II photoinitiating systems. The reactivity of MACSs both as additives for Type I PIs and as coinitiators (coI) in Type II photoinitiating systems in FRP will be studied, and the role of the central atom will be investigated. The experiments will be carried out under air in a low viscosity and relatively thin monomer film and upon a low incident light energy: these are the worst conditions for a photopolymerization reaction. The involved mechanisms will be discussed in detail.

Materials

The compounds shown in Scheme 3, tetrakis(dimethylamido)-silane (**Si**), tetrakis(dimethylamido)tin(IV) (**Sn**), tetrakis(dimethylamido)titanium(IV) (**Ti(1)**), tetrakis(diethylamido)titanium-(IV) (**Ti(2)**), tetrakis(dimethylamido)zirconium(IV) (**Zr**), and 1,3,5-triaza-7-phosphaadamantane (**P**), were purchased from Aldrich and used with the best purity available. Benzophenone (**BP**) is used as a Type II PI (Aldrich). For comparison, ethyldimethylaminobenzoate (**EDB** − Esacure **EDB** from Lamberti) or methyldiethanolamine (Aldrich) was chosen as reference amine coinitiator. Phenyl bis(2,4,6-trimethylbenzoyl)phosphine oxide (**BAPO** from Ciba), 2-hydroxy-2-methyl-1-phenyl-1-propanone (**HMPP**, Darocur 1173 from Ciba), 2,4,6-trimethylbenzoyl-diphenyl phosphine (**TPO**, Ciba), and 2,2-dimethoxy-2-phenyl acetophenone (**DMPA**, Irgacur 651 from Ciba or Esacure KB1 from Lamberti) were used as Type I PIs. Eosin-Y, 4,4′-bis(diethylamino)-benzophenone (**EAB**), isopropylthioxanthone (**ITX**), camphorquinone (**CQ**), and bis[2-(*o*-chlorophenyl)-4,5-diphenylimidazole] (**Cl-HABI**) were used in visible light photosensitive formulations.

Experimental Section

i. Photopolymerization Experiments. For film polymerization experiments, TMPTA (trimethylolpropane triacrylate from Cytec) was used as a low viscosity monomer (100 cP). Some experiments using an ethoxylated pentaerythritol tetraacrylate (EPT from Cray Valley; 150 cP) were also carried out. The PIs (1% w/w; excepted otherwise indicated) were dissolved in these media.

To avoid any degradation of MACSs during the preparation of the formulation, a direct injection into the monomer medium (or a preparation of the samples under argon) has been used. To get a good reproducibility, thin samples with low PI optical densities were used. These experimental conditions allow a good dissipation of the heat produced during the polymerization reaction and avoid any internal filter effects.[10,17−19] The experiments were carried out both in laminated and under air conditions. Some typical conversion versus irradiation time plots are given Figures 1−4.

The films (20 μm thick) deposited on a BaF_2 pellet were irradiated with either the polychromatic light or a monochromatic filtered light (365 nm) provided by a Xe−Hg lamp (Hamamatsu, L8252, 150 W) or with an LED (405 nm; cube−continuum). The evolution of the double-bond content was continuously followed by real-time FTIR spectroscopy (Nexus 870, Nicolet) at ∼1630 cm^{-1}.[10,17−19] The Rp quantities refer to the maximum rates of the polymerization reaction and were calculated from the maximum of the first derivative of the conversion versus time curves.

ii. Laser Flash Photolysis Experiments. Nanosecond laser flash photolysis (LFP) experiments were carried out using a Q-switched nanosecond Nd/YAG laser (λ_{exc} = 355 nm, 9 ns pulses; energy reduced down to 10 mJ, from Powerlite 9010 Continuum) and an analyzing system consisting of a pulsed xenon lamp, a monochromator, a fast photomultiplier, and a transient digitizer.[20]

iii. Kinetic ESR. The ESR experiments were carried out using a X-band spectrometer (MS 200 from Magnettech-Berlin; Germany) at RT. The *t*-Bu-$OO^{\bullet}$ radical was formed from the photolysis of 2,2,4,4-tetramethylpent-3-one in an oxygenated solvent (*tert*-butylbenzene). During the photolysis, the spectrometer was set at the magnetic field corresponding to the maximum peak height of the first derivative of the observed radical, and the field sweep was switched off. The decays of the signal were monitored when the light was off. The kinetic ESR (KESR) procedures have been described in detail in ref 21. The interaction rate constants of a model peroxyl (tBu-$OO^{\bullet}$) with MACSs were determined from the lifetime of tBu-$OO^{\bullet}$ at different quencher concentrations through classical Stern−Volmer plots.

iv. Density Functional Theory Calculations. All calculations were performed using the hybrid functional B3LYP from the Gaussian 03 suite of program.[22]. Reactants and products were fully optimized at the UB3LYP/LANL2DZ level and frequency checked.

Results and Discussion

1. Thermal Stability of MACSs in Formulations. Although such MACS compounds are usually characterized by a high sensitivity to oxygen and humidity (except **Si** which is highly stable), some of them show a remarkable stability in the monomer medium for several days. It has been observed that the central atom plays a crucial role in their stability versus the oxygen and the water dissolved in the polymer matrix. Compounds **Si**, **Ti(2)**, **Zr**, and **P** appeared to be the most stable, which makes their storage easy. The other compounds (**Sn** and **Ti(1)**) exhibited high O_2 and H_2O sensitivity, which leads to a fast degradation of the formulations. This lack of stability prevented the use of these compounds in photopolymerization studies.

The substituent (e.g., for **Ti(1)** vs **Ti(2)**) could also play an important role in their stability. **Ti(1)** is unstable because a high exothermic thermal polymerization reaction has been observed in the formulation at RT (preventing any storage). **Ti(2)** has shown excellent stability in the polymer matrix for several days after the preparation. This stability is attributed to the coordination of Ti(IV) with the monomer carbonyl group. Such kind of behavior has been already encountered in other previous works;[23] it also outlines the important effect of the substituents: methyls for **Ti(1)** versus ethyls for **Ti(2)**. A noticeable steric effect can be invoked.

2. Additive Effect of MACSs in Type I Photoinitiating Systems (BAPO, HMPP, and DMPA). BAPO, **HMPP**,

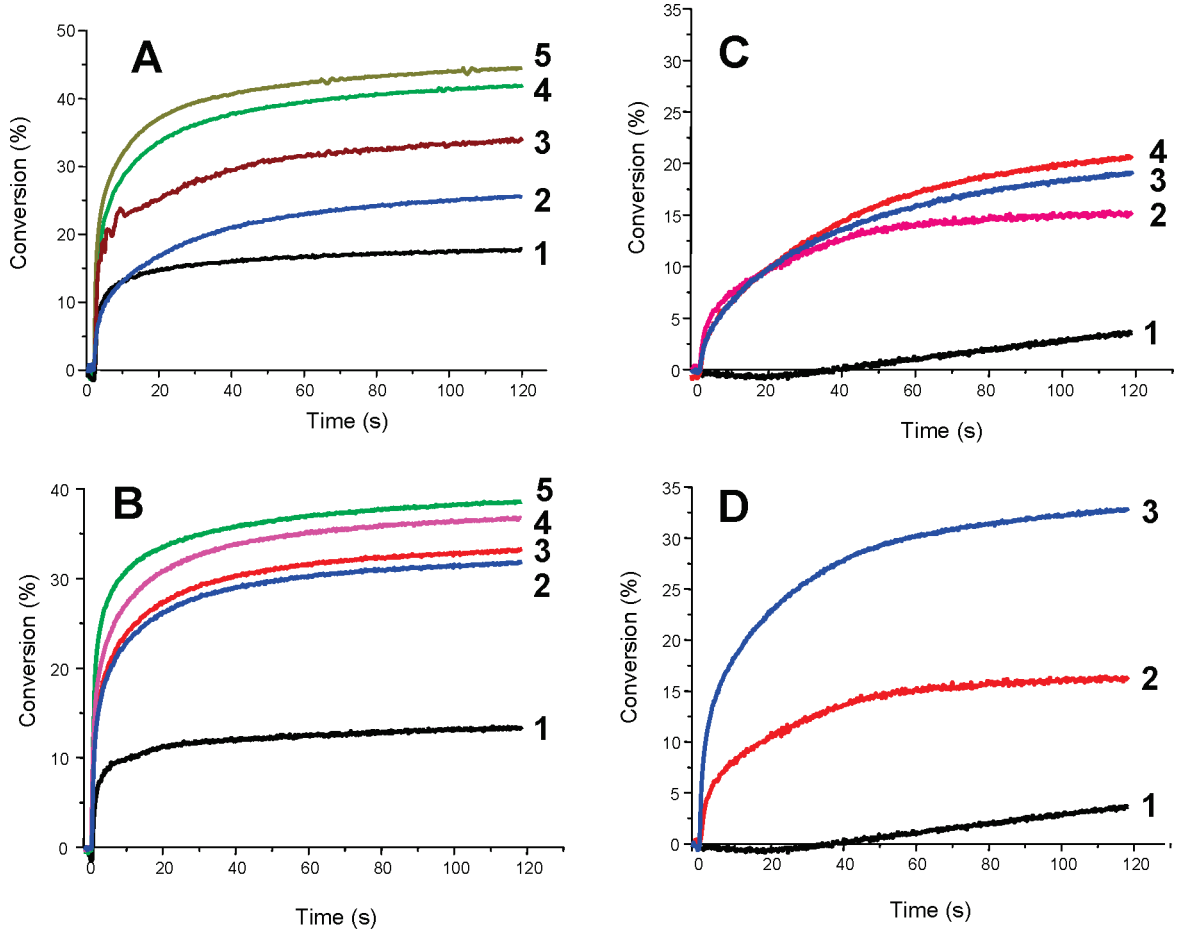

Figure 1. Photopolymerization of trimethylolpropane triacrylate under air in the presence of (A) 2,2-dimethoxy-2-phenyl acetophenone/**additive**: (1) without additive; (2) methyldiethanolamine; (3) tris(trimethylsilyl)silane; (4) tetrakis(diethylamido)titanium(IV); (5) tetrakis(dimethylamido)silane (Hg−Xe lamp; I_0 = 22 mW cm^{-2}; additive: 3% w/w). (B) Phenyl bis(2,4,6-trimethylbenzoyl)phosphine oxide/**additive**: (1) without additive; (2) tetrakis(diethylamido)titanium(IV); (3) tetrakis(dimethylamido)zirconium(IV); (4) 1,3,5-triaza-7-phosphaadamantane; (5) tetrakis(dimethylamido)-silane (Hg−Xe lamp; λ = 365 nm; $I_0 \approx$ 3.5 mW cm^{-2}; additive: 1% w/w). (C) 2-Hydroxy-2-methyl-1-phenyl-1-propanone/**additive**: (1) without additive; (2) tetrakis(dimethylamido)silane; (3) tetrakis(diethylamido)titanium(IV); (4) tetrakis(dimethylamido)zirconium(IV) (Hg−Xe lamp; I_0 = 22 mW cm^{-2}; additive: 1% w/w). (D) 2-Hydroxy-2-methyl-1-phenyl-1-propanone/**additive**: (1) without additive; (2) tetrakis(dimethylamido)silane (1% w/w); (2) tetrakis(dimethylamido)silane (3% w/w) (Hg−Xe lamp; I_0 = 22 mW cm^{-2}).

and **DMPA** are efficient but very oxygen-sensitive PIs for the photopolymerization of acrylate monomers. Under the conditions chosen here (low viscosity, low intensity, and relatively thin samples), the strong oxygen inhibition is revealed by the low final conversions of ~15, 12, and < 5% obtained when using **DMPA**, **BAPO**, and **HMPP** alone, respectively (Figure 1). Interestingly, the addition of MACSs to these PIs allows a significant increase in both the polymerization rates and the final conversions under air (Figure 1). For example, the final conversions are increased by a three-fold factor through the addition of **Si** to **DMPA** and **BAPO**. For **HMPP**, significant conversions are only reached in the presence of these additives.

An increase in the photopolymerization efficiency was also observed upon increasing the MACS concentration (Figure 1D). No additive effect is noted when replacing the amino groups by isopropoxide substituents, for example, by using titanium(IV) isopropoxide. This behavior that is ascribed to a low efficiency of the S_H2 reaction for this compound will be discussed below.

The additive effect of MACSs was also compared with those of silanes or amines.[24] Interestingly, it is clearly noted (Figure 1A) that both the silane and MACS lead to much better additive effects than the amines (methyldiethanolamine). The properties of MACSs are highly valuable and lead to better polymerization kinetics than those obtained with the recently proposed tris(trimethylsilyl)silane.[24]

3. Role of MACSs as coI in Type II Photoinitiating Systems. The photoinitiating abilities of **MACSs** as coI were checked both in laminate and under air and compared with those of the well-known **BP/EDB** Type II PI system (Figure 2, Table 1). The **BP/MACS** systems appear to be highly efficient for the photopolymerization of TMPTA and better than the **BP/EDB** reference. The most dramatic effect is observed under air where **BP/EDB** almost does not work: the addition of **Zr** to **BP** increases the final conversion by a ~5-fold factor (from 10.7 to 49.3%) and increases the polymerization rates by a ~100-fold factor (going from 0.2 to 20.8 s^{-1}), leading to a tack-free coating. This is evidence of MACSs also working as efficient coinitiators in photopolymerization under aerated conditions. **Ti(2)** and **Zr** are the most powerful coIs. Figure 3 shows the noticeable higher efficiency of **Ti(2)** compared with **EDB** when adjusting the coI concentration to have the same number of labile α(C−H) hydrogen atoms: this confirms the specific behavior of these compounds under air.

4. Photopolymerization under a LED at 405 nm. The development of FRP under a monochromatic visible light using a LED is important for potential applications. FRP of samples with low thickness under air with such an irradiation

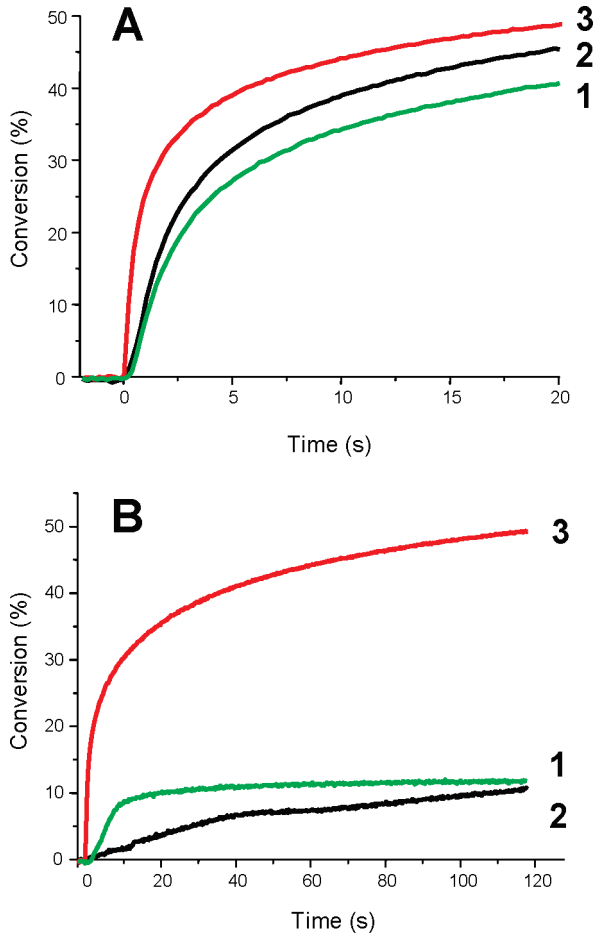

Figure 2. Conversion versus time curves for the photopolymerization of trimethylolpropane triacrylate. Photoinitiating system: benzophenone/**coI** 1/1% w/w. (A) In laminate with coI = 1,3,5-triaza-7-phosphaadamantane (1), ethyldimethylaminobenzoate (2), and tetrakis-(dimethylamido)zirconium(IV) (3). (B) Under air. Hg−Xe lamp; I_0 = 44 mW cm^{-2}.

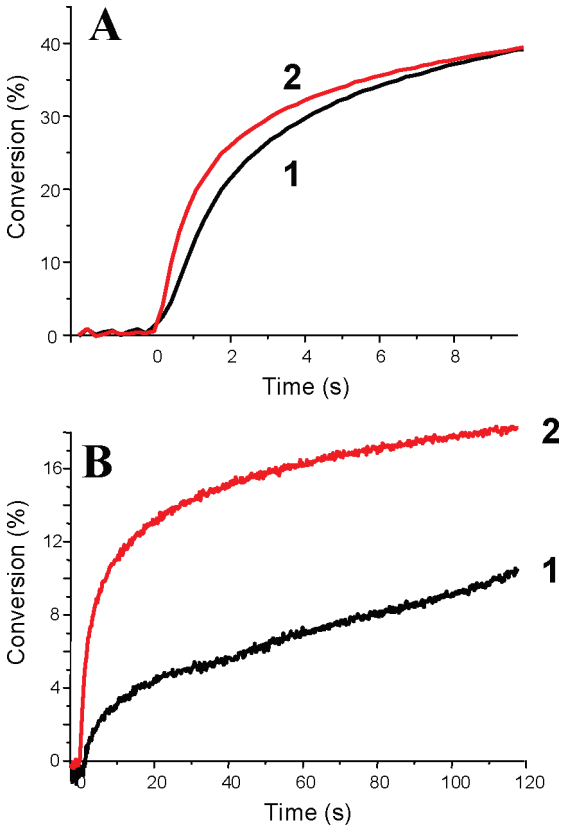

Figure 3. Concentration effects in the conversion versus time curves for the photopolymerization of trimethylolpropane triacrylate. Photoinitiating system: (1) benzophenone/ethyldimethylaminobenzoate (1/1.7% w/w) and (2) benzophenone/tetrakis(diethylamido)titanium(IV) (1/0.8% w/w). (A) In laminate and (B) under air; Hg−Xe lamp; I_0 = 44 mW cm^{-2}.

device is, however, usually limited by the oxygen inhibition effect. As seen in Figure 4, the polymerization of TMPTA using the **CQ/Si** photoinitiating system under air is much more efficient than that in the presence of the **CQ/EDB** reference, whereas it exhibits a quite close efficiency under laminated conditions. A significant improvement in Type I systems is also observed, for example, when **Si** is added to **BAPO**. These results confirm what was reported above and show the high performance of these new proposed systems. Interestingly, for a quite low energy (8 mW cm^{-2}), the addition of **Si** to **TPO** (Figure 4C) increases both the final conversion (~1.8 fold factor; from 35 to 62%) and the polymerization rates (~2.4 fold factor; from 0.118 to 0.288 s^{-1}) and leads to a tack-free coating. Without the additives, the films remained very tacky, as expected from the low final conversion. As previously, **Si** is a very interesting compound that leads to slightly better polymerization kinetics than those obtained with the recently proposed tris(trimethylsilyl)silane (Figure 4C).[24]

5. Formation and Reactivity of the Aminoalkyl Radicals Derived from MACSs. The interaction rate constants of the benzophenone triplet state with the MACSs (as well as the ketyl radical quantum yields) were measured by LFP (Table 2). The very high rate constants are in agreement with an electron transfer, followed by a proton transfer process typical of classical amines.[20] The aminoalkyl radical derived from **Si** (Y$^\bullet$) was also observed (Figure 5) using a hydrogen abstraction reaction between the *tert*-butoxyl radical *t*-BuO$^\bullet$ (generated via the direct cleavage of di-*tert*-butylperoxide) and **Si**. Interestingly, Y$^\bullet$ is characterized by a quite high addition rate constant to methylacrylate (1.6×10^6 M^{-1} s^{-1}), thereby demonstrating that this structure is very efficient to initiate a polymerization. This value is higher than that reported for the EDB-derived aminoalkyl radical (5×10^5 M^{-1} s^{-1}).[25] The other MACS-derived aminoalkyl radicals were not characterized because of their lack of stability in organic solvents under air. However, their electronic structures were determined by molecular orbital calculations (Table 2, Figure 6). High spin densities (SDs) for the carbon radical center are found (Table 2), even if they are a little reduced for **Zr** (0.82) and **Ti(2)** (0.73) compared with **Si** (0.9). On the basis of these quite high SDs, an important initiation efficiency of the corresponding radicals is expected.

6. Reactivity of MACSs with Peroxyl Radicals. The interaction rate constants of MACSs with a model peroxyl (*t*-BuOO$^\bullet$) were determined by Kinetic ESR (Figure 7). The interaction rate constants of the **ROO$^\bullet$/coI** for **coI** = **Si**, **Ti(2)**, and **P** are 130, 400, and 400 M^{-1} s^{-1} respectively. that is, noticeably higher compared with $k \approx 6$ M^{-1} s^{-1} for **ROO$^\bullet$/EDB**. On the basis of the calculated α(C−H) bond dissociation energies (BDEs) (gathered in Table 2), which are slightly higher for MACSs than for the reference EDB, low hydrogen abstraction rate constants are expected. Therefore, the enhanced reactivity of MACSs demonstrates that the ROO$^\bullet$/MACS interaction is not a hydrogen abstraction

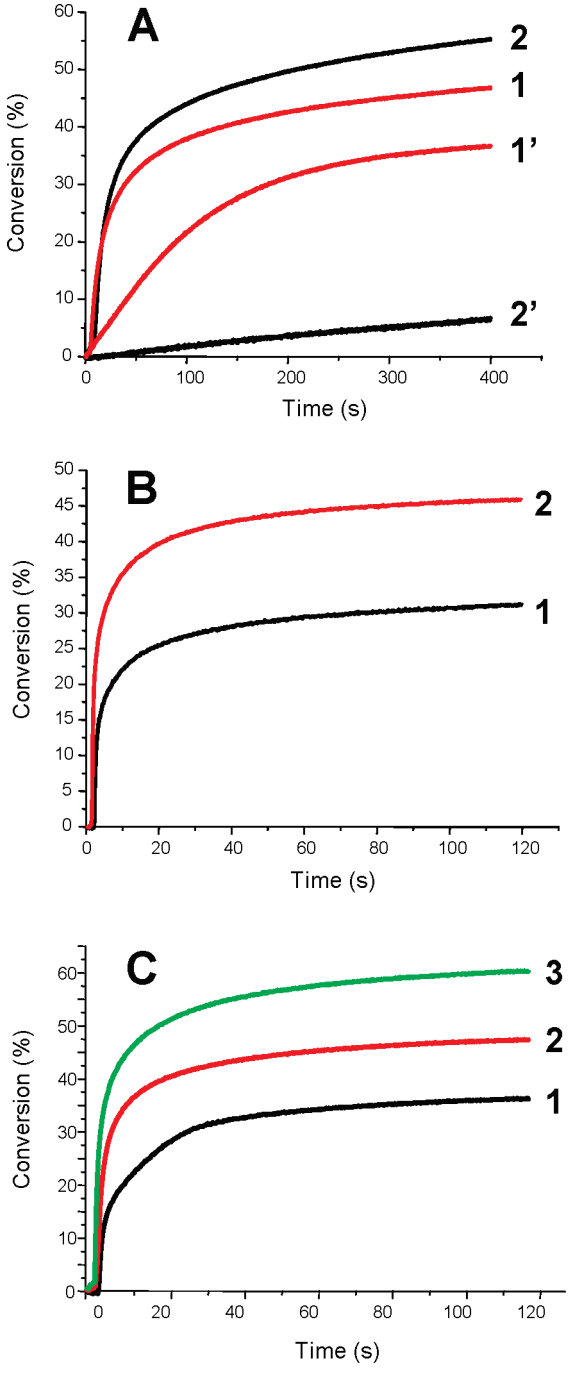

Figure 4. Photopolymerization of trimethylolpropane triacrylate under monochromatic irradiation (LED: λ = 405 nm; I_0 = 8 mW cm^{-2}). Photoinitiating systems: (A) Camphorquinone/ethyldimethylaminobenzoate (3/3% w/w) in laminate (2) and under air (2′) conditions and camphorquinone/tetrakis(dimethylamido)silane (3/3% w/w) in laminate (1) and under air (1′). (B) Photopolymerization of trimethylolpropane triacrylate under air in the presence of (1) Phenyl bis(2,4,6-trimethylbenzoyl)phosphine oxide (3% w/w) and (2) phenyl bis(2,4,6-trimethylbenzoyl)phosphine oxide/tetrakis(dimethylamido)silane (3/3% w/w). (C) Photopolymerization of EPT under air in the presence of (1) 2,4,6-trimethylbenzoyl-diphenyl phosphine (1% w/w), (2) 2,4,6-trimethylbenzoyl-diphenyl phosphine/tris(trimethylsilyl)silane (1/3% w/w), and (3) 2,4,6-trimethylbenzoyl-diphenyl phosphine/tetrakis-(dimethylamido)silane (1/3% w/w).

(Scheme 1) but an S_H2 reaction (Scheme 2). The addition reaction enthalpies were calculated at the UB3LYP/LANL2DZ level as −2.2, −36, and −51 kJ/mol for **Si**; **Ti(2)**, and **Zr**, respectively, in line with the measured high rate

Table 1. Polymerization Rates of Trimethylolpropane Triacrylate (TMPTA) using a Benzophenone/Multivalent Atom Containing Structure (BP/MACS) Type II Photoinitiating System (1/1%, w/w)[a]

	laminate		under air	
	Rp/[M$_0$] × 100 (s^{-1})	conversion (%)	Rp/[M$_0$] × 100 (s^{-1})	conversion (%)
EDB[b]	12.7	60.6	0.2	10.7
Si	15.6	57.2	7.1	13.2
Ti(2)	22.1	48.0	17.4	27.5
Zr	38.5	61.6	20.8	49.3
P	11.1	55.9	1.3	11.8

[a] Xenon-Hg lamp. I_0 = 44 mW cm^{-2}. [b] Ethyldimethylaminobenzoate.

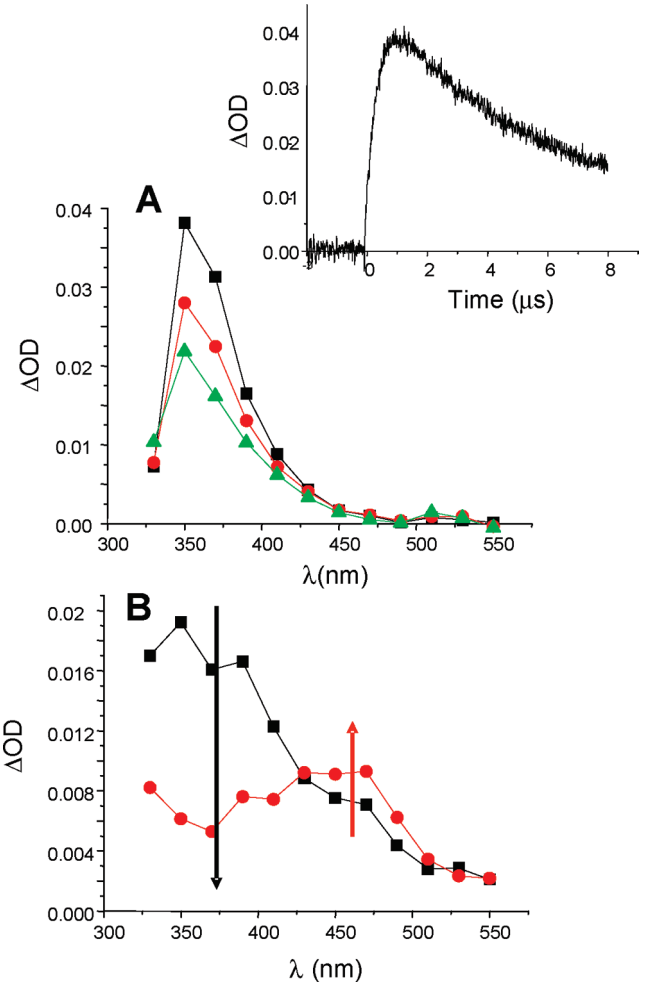

Figure 5. (A) Absorption spectra of the aminoalkyl radical of **Si** in di-*tert*-butylperoxide ([tetrakis(dimethylamido)silane] = 0.02 M) at time = 0.9 (■), 2.3 (●), and 4.6 μs (▲) after excitation. Insert: kinetic observed at 340 nm. (B) Evolution of the absorption spectra in the presence of 0.4 M methylacrylate (MA): decay (■) of the aminoalkyl radical (λ_{max} = 350 nm, t = 0.5 μs) and rise (●) of the acrylate radical at 470 nm (t = 13 μs).

constants: for example, the exothermicity is higher for **Ti(2)** than for **Si**, which is in full agreement with the higher interaction rate constant found for **Ti(2)**. For titanium(IV) isopropoxide, the reaction is endothermic (90 kJ/mol) and hence unfavorable. This is in agreement with the low additive effect of this compound in photopolymerization under aerated conditions (see above).

7. Involved Mechanisms. According to Scheme 4, primary radicals R′• are generated from the fast cleavage of type I PIs (**BAPO**: substituted phosphinoyl and benzoyl radicals from

Table 2. Interaction Rate Constants with ^{3}BP (k_q) and tBuOO$^\bullet$ (k), Quantum Yield for Ketyl Radical Formation (Φ_K), Bond Dissociation Energies (BDEs) of the α(CH) Bond, and Spin Densities (SDs) on the Carbon Radical Center for the Aminoalkyl Radicals Derived from MACSs[a]

	BP[b]		*t*-Bu-OO$^\bullet$	BDE (kcal/mol)[c]	SD
	k_q (M^{-1} s^{-1}) 10^7	Φ_K	k (M^{-1} s^{-1})	α(CH)	C$^\bullet$
EDB[d]	510[e]	1.0[e]	6	92.0	
Si	750	0.95	130	94.5	0.9
Sn	[f]			95.3	0.9
Ti (1)	[f]			92.0	0.73
Ti (2)	600	0.9	400	91.5	
Zr	[f]			94.1	0.82
P	1000	0.1	400	93.8[g] (97.4)[h]	0.97

[a] See the text. [b] In *tert*-benzene. [c] Calculations at UB3LYP/LANL2DZ level. [d] Ethyldimethylaminobenzoate. [e] From ref 25. [f] Not stable enough in the solvent. [g] P−C**H**-N. [h] N−C**H**-N.

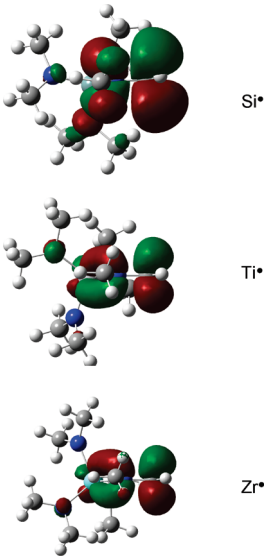

Figure 6. Optimized structures and SOMO orbitals of the aminoalkyl radicals derived from tetrakis(dimethylamido)silane, tetrakis(dimethylamido)titanium(IV), and tetrakis(dimethylamido)zirconium(IV).

a C−P bond cleavage; **HMPP**: benzoyl and 2-hydroxyisopropyl radicals from a C−C cleavage; **DMPA**: benzoyl and dimethoxybenzyl radicals from a C−C cleavage) in their short-lived triplet state, which prevents almost any quenching by oxygen or monomer. In BP/coI (Type II PIs), a fast hydrogen transfer occurs between ^{3}BP and coI (Table 2): ketyl K$^\bullet$ and aminoalkyl radicals (Y$^\bullet$ in Scheme 4; reaction ii) are formed. In Scheme 4, the same set of reactions holds true for type II systems with Y$^\bullet$ = R′$^\bullet$. All of these radicals (generated from Type I or Type II systems) either react with the monomer (except K$^\bullet$) or are deactivated by oxygen to form peroxyl radicals. This oxygen quenching also occurs for the propagating radicals (R′$M_n^\bullet$) and efficiently competes, in TMPTA, with the propagation step (k_p[monomer] ≈ 3×10^4 s^{-1} < k_{O_2}[O_2] ≈ 2.1×10^5 s^{-1}). When nothing is added, an important Rp decrease is observed as peroxyl radicals are mainly present on the time scale of the experiment.[24] The possible interaction between the R′$^\bullet$ radicals and **MACS** should not compete; that is, for example, the interaction rate constant between MesC(═O)Ph(O═)P• (**BAPO** phosphinoyl radical) and **Si** is lower than 5×10^5 M^{-1} s^{-1} versus 2×10^7 and 3×10^9 M^{-1} s^{-1} for the MesC(═O)Ph(O═)P•/monomer and MesC(═O)Ph(O═)P•/O_2 interactions, respectively.

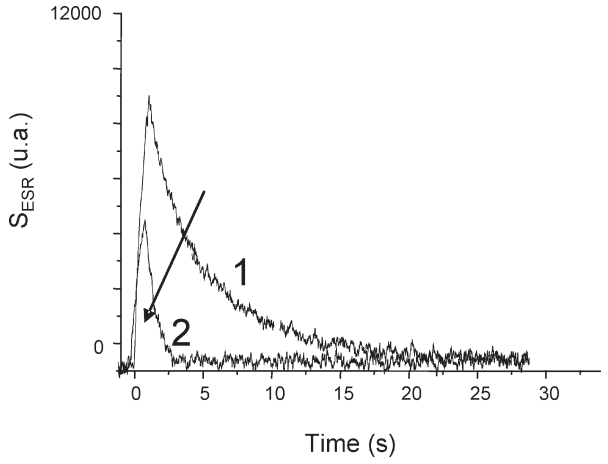

Figure 7. ESR decay of the peroxyl radical (tBuOO$^\bullet$) before (1) and after (2) the addition of tetrakis(diethylamido)titanium(IV).

Scheme 4. Proposed Mechanism

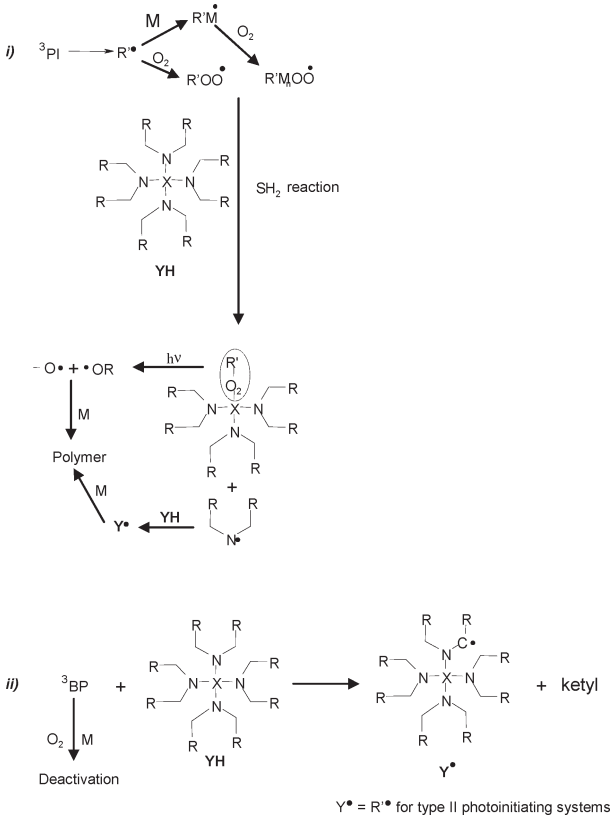

Therefore, the increase in the photopolymerization efficiency under air can be explained on the basis of Scheme 4, which involves several driving processes:

(1) A remarkable efficient addition reaction of the aminoalkyl radical to oxygen (Figure 5) is found here in the case of **Si** (a high rate constant of $2-4 \times 10^9$ M^{-1} s^{-1} close to the diffusion limit is measured). This is in agreement with the rate constants found for other aminoalkyls in ref 25. This process ensures a fast consumption of O_2 for the BP/coI systems.

(2) The S_H2 reactions[16,29−31] are likely the main processes: it corresponds to the addition of a peroxyl to a MACS compound (except with **P**), which results in an aminyl radical and a MACS peroxide (Scheme 4).

Scheme 5. Phosphoranyl Pathway

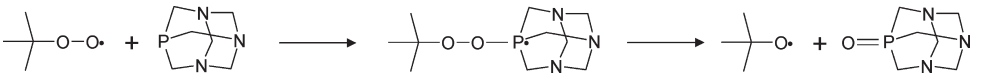

Table 3. Polymerization Rates of Trimethylolpropane Triacrylate in Laminate (L) and under Air (A) in the Presence of (i) Isopropylthioxanthone/coI (1/1%, w/w); Hg−Xe Lamp; I_0 = 22 mW cm^{-2}, (ii) Bis[2-(*o*-chlorophenyl)-4,5-diphenylimidazole]/coI (1/3% w/w), Benzophenone/bis[2-(*o*-chlorophenyl)-4,5-diphenylimidazole]/coI (1/1/3%w/w); Hg−Xe Lamp; I_0 = 44 mW cm^{-2}, (iii) 4,4′-Bis(diethylamino)-benzophenone/bis[2-(*o*-chlorophenyl)-4,5-diphenylimidazole]/coI (0.1/1/3% w/w); Hg−Xe Lamp; I_0 = 44 mW cm^{-2}, and (iv) Camphorquinone/bis[2-(*o*-chlorophenyl)-4,5-diphenylimidazole]/coI (3/1/3% w/w); Xenon Lamp at λ > 400 nm; $I_0 \approx$ 40 mW cm^{-2}[a]

	ITX/CoI		Cl-HABI/coI		BP/Cl-HABI/coI		EAB/Cl-HABI/coI	CQ/Cl-HABI/coI
	L[b]	A[c]	L[b]	A[c]	L[b]	A[c]	A[c]	A[c]
	Rp/[M$_0$] s^{-1}	Rp/[M$_0$] s^{-1}	Rp/[M$_0$] s^{-1}	Rp/[M$_0$] s^{-1}	Rp/[M$_0$] s^{-1}	Rp/[M$_0$] s^{-1}	Rp/[M$_0$] s^{-1}	Rp/[M$_0$] s^{-1}
EDB[d]	0.51	0.37	0.016 (41)	0.001 (9)	9.0 (63)	0.008 (32)	0.024 (20)	0.07 (54)
Si	0.54	0.53	0.043 (58)	0.005 (19)	3.2 (57)	0.054 (38)	0.071 (34)	0.113 (36)
Ti(2)	0.49	0.44	0.024 (54)	0.006 (26)	14.3 (64)	0.072 (55)	0.035 (28)	0.07 (23)

[a] The final conversions are given in brackets. [b] Laminated conditions. [c] Under air. [d] Ethyldimethylaminobenzoate.

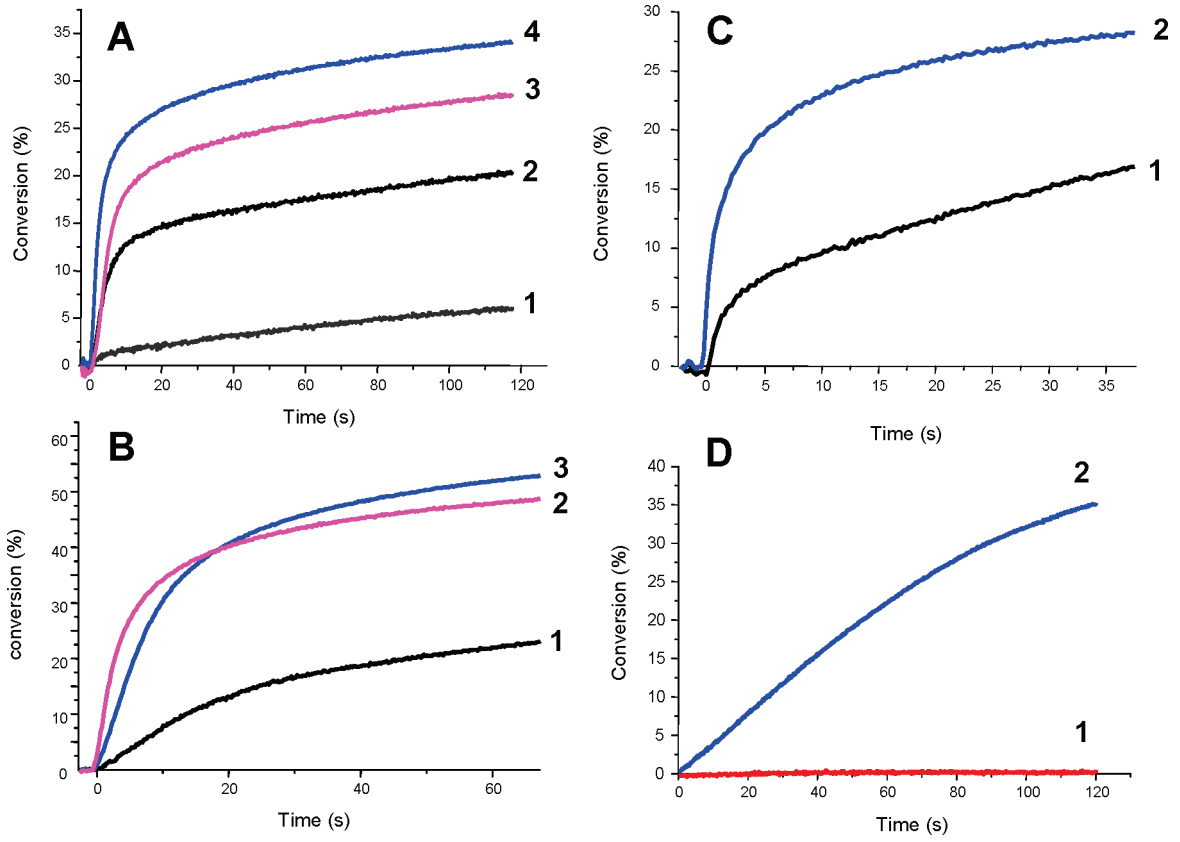

Figure 8. (A) Conversion versus time curves for the photopolymerization of trimethylolpropane triacrylate under air in the presence of various photoinitiating systems. (A) 4,4′-Bis(diethylamino)-benzophenone/bis[2-(*o*-chlorophenyl)-4,5-diphenylimidazole]/**coI** 0.1/1/3% w/w); Hg−Xe lamp; I_0 = 44 mW cm^{-2}: (1) without coI, (2) ethyldimethylaminobenzoate, (3) tetrakis(diethylamido)titanium(IV), and (4) tetrakis(dimethylamido)silane. (B) Benzophenone/bis[2-(*o*-chlorophenyl)-4,5-diphenylimidazole]/**coI** (1/1/3% w/w); Hg−Xe lamp; I_0 = 44 mW cm^{-2}: (1) EDB, (2) tetrakis-(diethylamido)titanium(IV), and (3) tetrakis(dimethylamido)silane. (C) Isopropylthioxanthone/**coI** (1/3% w/w); Hg−Xe lamp; λ_{exc} = 365 nm; $I_0 \approx 1$ mW/cm^2: (1) ethyldimethylaminobenzoate and (2) tetrakis(dimethylamido)silane. (D) Eosin-Y/**coI** (0.05/3% w/w); xenon lamp; λ_{exc} > 400 nm; $I_0 \approx 40$ mW/cm^2: (1) ethyldimethylaminobenzoate and (2) tetrakis(dimethylamido)silane.

The aminyl (which is not a good initiating structure[26]) fortunately further reacts with MACS to form an aminoalkyl, which is a highly efficient initiating radical.[27] This process is quite favorable because the (N−H) BDE is ~96 kcal/mol and the α(C−H) BDE of MACSs is ~91−94 kcal/mol, in agreement with an exothermic hydrogen abstraction reaction. In the case of **P**, the addition of the peroxyl to the trivalent phosphorus atom leads to a phosphoranyl radical (Scheme 5). This latter should not be stable, as revealed by molecular orbital calculations (UB3LYP/6-31G* level): it undergoes the formation of an alkoxyl radical, which can initiate the photopolymerization. Such a process was already evidenced in another trivalent phosphorus compound.[28]

(3) The photodecomposition of the peroxides generated in the S_H2 reaction can also contribute to some extent. Indeed, as generally observed, peroxides and hydroperoxides cleave under polychromatic irradiation and create new initiating oxyl and hydroxyl radicals.[32]

8. MACSs in Other Photosensitive Systems For UV or Visible Light Irradiations. Additional experiments have been carried out to outline the role and the potential of two particular MACSs (**Si** and **Ti(2)**) in various near-UV or visible light photosensitive systems based on (i) ITX and Eosin-Y and (ii) different combinations containing Cl-HABI, which is a well-known compound largely used in the laser imaging science area.[1−5] The results reported in Table 3 and the typical conversion−time curves displayed in Figure 8 support the interest of these systems for achieving an efficient photopolymerization of a low-viscosity monomer in thin film, in aerated media, under quite low light intensities, and even in the visible wavelength range. **Si** and **Ti(2)** are clearly better coinitiators/additives than EDB for all of the selected experimental photopolymerization conditions. **ITX/Si** presumably behaves as **BP/Si**. The high efficiency of Eosin/**Si** (no monomer conversion is found when using Eosin/EDB) could be ascribed to the additive effect of **Si** through the S_H2 reaction. The behavior of **EAB** (or **BP**)/**Cl-HABI/Si** lies on a complex set of reactions involving the direct **EAB** (or **BP**)/**Cl-HABI** interaction, as observed in other three-component systems and discussed elsewhere,[33] a specific **EAB** (or **BP**)/**Si** interaction, and also presumably by-side reactions originating from the generated radicals (ketyl, lophyl, etc.) with **Si**.

Conclusions

The proposed MACSs involving multivalent atom-containing amines show a photopolymerization ability in Type I and Type II systems higher than that of a reference both in laminate and under air. The striking and outstanding enhanced performance under air is accounted for by a S_H2 reaction that appears as a new way to reduce the oxygen inhibition as long as a suitable $ROO^{\bullet}$/additive couple is defined. This could open up a new approach for the design of high-performance systems usable in the radiation curing and laser imaging science areas. Such a S_H2 reaction involving peroxyls and suitable compounds might also be of interest in other fields, such as in the photostabilization of polymers.

References and Notes

(1) (a) Fouassier, J. P. *Photoinitiation, Photopolymerization, and Photocuring: Fundamental and Applications*; Hanser Publishers: New York, 1995. (b) Fouassier, J. P. In *Radiation Curing in Polymer Science and Technology*; Fouassier, J. P., Rabek, J. F., Eds.; Elsevier Science Publishers: London, 1993. (c) *Photochemistry and UV Curing*; Fouassier, J. P., Ed.; Research Signpost: Trivandrum, India, 2006. (d) *Basics and Applications of Photopolymerization Reactions*; Fouassier, J. P., Allonas, X., Eds.; Research Signpost: Trivandrum, India, in press.

(2) Pappas, S. P. *UV Curing Science and Technology*; Technology Marketing Corp.: Stamford, CT, 1978.

(3) Dietliker, K. *Chemistry & Technology of UV & EB Formulation for Coatings, Inks, & Paints*; SITA Technology: London, 1991.

(4) (a) Davidson, R. S. *Exploring the Science, Technology, and Applications of UV and EB Curing*; SITA Technology: London, 1999. (b) Schwalm, R. *UV Coatings: Basics, Recent Developments, and New Applications*; Elsevier: Oxford, U.K., 2007

(5) (a) *Photoresponsive Polymers*; Krongauz, V., Trifunac, A., Eds.; Chapman and Hall: New York, 1994. (b) Neckers, D. C. *UV and EB at the Millenium*; Sita Technology: London, 1999. (c) Reiser, A. *Photoreactive Polymers: The Science and Technology of Resists*; Wiley: New York, 1989.

(6) (a) Hoyle, C. E.; Kim, K.-J. *J. Radiat. Curing* **1985**, 9–15. (b) Decker, C.; Jenkins, A. D. *Macromolecules* **1985**, *18*, 1241–1244. (c) Andrzejewska, E.; Zych-Tomkoviak, D.; Andrezejewski, M.; Hug, G. L.; Marciniak, B. *Macromolecules* **2006**, *93*, 3777–3785.

(7) Krongauz, V. V.; Chawla, C. P.; Dupre, J. In *Photoinitiated Polymerization*; Belfield, K., Crivello, J. V., Eds.; ACS Symposium 847; American Chemical Society: Washington, DC, 2003.

(8) Decker, C. *Makromol. Chem., Macromol. Chem. Phys.* **1979**, *180*, 2027–2030.

(9) Miller, C. W.; Hoyle, C. E.; Jonsson, S.; Nason, C.; Lee, T. Y.; Kuang, W. F.; Viswanathan, K. In *Photoinitiated Polymerization*; Belfield, K., Crivello, J. V., Eds; ACS Symposium 847; American Chemical Society: Washington, DC, 2003.

(10) (a) Lalevée, J.; Dirani, A.; El-Roz, M.; Allonas, X.; Fouassier, J. P. *Macromolecules* **2008**, *41*, 2003–2010. (b) Lalevée, J.; Blanchard, N.; Graff, B.; Allonas, X.; Fouassier, J. P. *J. Organomet. Chem.* **2008**, *693*, 3643–3649.

(11) Lalevée, J.; Blanchard, N.; El-Roz, M.; Graff, B.; Allonas, X.; Fouassier, J. P. *Macromolecules* **2008**, *41*, 4180–4186.

(12) Decker, C.; Faure, J.; Fizet, M.; Rychla, L. *Photogr. Sci. Eng.* **1979**, *23*, 137–140.

(13) (a) Davidson, R. S. In *Radiation Curing in Polymer Science and Technology*; Fouassier, J. P., Rabek, J. F., Eds.; Elsevier Science Publishers: London, 1993. (b) Jacobine, A. T. In *Radiation Curing in Polymer Science and Technology*; Fouassier, J. P., Rabek, J. F., Eds.; Elsevier Science Publishers: London, 1993. (c) Gush, D. P.; Ketley, A. D. *Mod. Paint. Coat.* **1978**, *68*, 61–72.

(14) Lecamp, L.; Houllier, F.; Youssef, B.; Bunel, C. *Polymer* **2001**, *42*, 2727–2736.

(15) Cramer, N. B.; Bowman, C. N. *J. Polym. Sci., Part A: Polym. Chem.* **2001**, *39*, 3311–3319.

(16) Ingold K. U.; Roberts, B. P. In *Free Radical Substitution Reactions*; Wiley Interscience: New York, 1971.

(17) El-Roz, M.; Lalevée, J.; Allonas, X.; Fouassier, J.-P. *Macromol. Rapid Commun.* **2008**, *29*, 804–808.

(18) Lalevée, J.; El-Roz, M.; Allonas, X.; Fouassier, J. P. *J. Polym. Sci., Part A: Polym. Chem.* **2008**, *46*, 2008–2014.

(19) Lalevée, J.; Allonas, X.; Jradi, S.; Fouassier, J.-P. *Macromolecules* **2006**, *39*, 1872–1879.

(20) Lalevée, J.; Allonas, X.; Fouassier, J. P. *J. Am. Chem. Soc.* **2002**, *124*, 9613–9621.

(21) (a) Furimsky, E.; Howard, J. A. *J. Am. Chem. Soc.* **1973**, *95*, 369–379. (b) Burton, B. W.; Doba, T.; Gabe, E. J.; Hughes, L.; Lee, F. L.; Prasad, L.; Ingold, K. U. *J. Am. Chem. Soc.* **1985**, *107*, 7053–7065. (c) Fukuzumi, S.; Shimoosako, K.; Suenobu, T.; Watanabe, Y. *J. Am. Chem. Soc.* **2003**, *125*, 9074–9082. (d) Griller, D.; Howard, J. A.; Marriott, P. R.; Scaiano, J. C. *J. Am. Chem. Soc.* **1981**, *103*, 619–623.

(22) (a) Frisch, M. J.; Trucks, G. W.; Schlegel, H. B.; Scuseria, G. E.; Robb, M. A.; Cheeseman, J. R.; Zakrzewski, V. G.; Montgomery, J. A., Jr.; Stratmann, R. E.; Burant, J. C.; Dapprich, S.; Millam, J. M.; Daniels, A. D.; Kudin, K. N.; Strain, M. C.; Farkas, O.; Tomasi, J.; Barone, V.; Cossi, M.; Cammi, R.; Mennucci, B.; Pomelli, C.; Adamo, C.; Clifford, S.; Ochterski, J.; Petersson, G. A.; Ayala, P. Y.; Cui, Q.; Morokuma, K.; Salvador, P.; Dannenberg, J. J.; Malick, D. K.; Rabuck, A. D.; Raghavachari, K.; Foresman, J. B.; Cioslowski, J.; Ortiz, J. V.; Baboul, A. G.; Stefanov, B. B.; Liu, G.; Liashenko, A.; Piskorz, P.; Komaromi, I.; Gomperts, R.; Martin, R. L.; Fox, D. J.; Keith, T.; Al-Laham, M. A.; Peng, C.Y.; Nanayakkara, A.; Challacombe, M.; Gill, P. M. W.; Johnson, B.; Chen, W.; Wong, M. W.; Andres, J. L.; Gonzalez, C.; Head-Gordon, M.; Replogle, E. S.; Pople, J. A. *GAUSSIAN 03*, revision B-2; Gaussian, Inc.: Pittsburgh, PA, 2003. (b) Foresman, J. B.; Frisch, A. In *Exploring Chemistry with Electronic Structure Methods*, 2nd ed.; Gaussian, Inc.: Pittsburgh, PA, 1996.

(23) (a) Mason, M. R.; Fneich, B. N.; Kirschbaum, K. *Inorg. Chem.* **2003**, *42*, 6592–6594. (b) Ward, D. B.; Risler, H.; Weitershans, K.; Bellemin-Laponnoz, S.; Wadepohl, H.; Gade, L. H. *Inorg. Chem.* **2006**, *45*, 7777–7787.

(24) El-Roz, M.; Lalevée, J.; Allonas, X.; Fouassier, J. P. *Macromolecules* **2009**, *42*, 8725–8732.

(25) Lalevée, J.; Graff, B.; Allonas, X.; Fouassier, J. P. *J. Phys. Chem. A* **2007**, *111*, 6991–6998.

(26) Lalevée, J.; Gigmes, D.; Bertin, D.; Graff, B.; Allonas, X.; Fouassier, J. P. *Chem. Phys. Lett.* **2007**, *438*, 346–350.

(27) Lalevée, J.; Allonas, X.; Genet, S.; Fouassier, J. P. *J. Am. Chem. Soc.* **2003**, *125*, 9377–9380.
(28) Lalevée, J.; Allonas, X.; Fouassier, J. P. *Chem. Phys. Lett.* **2007**, *445*, 62–67.
(29) Davies, A. G.; Roberts, B. P. In *Free Radicals*; Kochi, J. K., Ed.; Wiley: New York, 1973.
(30) Davies, A. G.; Roberts, B. P. *J. Chem. Soc. B* **1971**, 1830–1837.
(31) Davies, A. G.; Griller, D.; Roberts, B. P. *J. Chem. Soc. B* **1971**, 1823–1829.
(32) (a) Rabek, J. F. *Mechanisms of Photophysical and Photochemical Reactions in Polymer: Theory and Practical Applications*; Wiley: New York, 1987. (b) Rabek, J. F. *Photostabilization of Polymers: Principles and Applications*; Elsevier: New York, 1990.
(33) Allonas, X.; Fouassier, J. P.; Kaji, M.; Murakami, S. *Photochem. Photobiol. Sci.* **2003**, *2*, 224–229.